Strain Measurement Using FBG on COPV in Stress Rupture Test

Prepared

By

Curtis Banks EV43 & Joseph Grant VP63

Outline

Introduction

White Sands Test Facility (WSTF) was requested to perform ambient temperature hydrostatic pressurization testing of a Space Transportation System (STS) 40-in. Kevlar®[1] Composite Overwrapped Pressure Vessel (COPV). The 40-in. vessel was of the same design and approximate age as the STS Main Propulsion System (MPS) and Orbiter Maneuvering System (OMS) vessels.

The NASA Engineering Safety Center (NESC) assembled a team of experts and conducted an assessment that involved a review of national Kevlar COPY data. During the review, the STS COPVs were found to be beyond their original certification of ten years. The team observed that the likelihood of STS COPV Stress rupture, a catastrophic burst before leak failure mode, was greater than previously believed. Consequently, a detailed assessment of remaining stress rupture life became necessary. Prior to STS-114, a certification deviation was written for two flights of OV-103 (Discovery) and OV-104 (Atlantis) per rationale that was based on an extensive review of the Lawrence Livermore National Laboratories, COPV data, and revisions to the STS COPV stress levels. In order to obtain flight rationale to extend the certification deviation through the end of the Program, the Orbiter Project Office has directed an interagency COPV team to conduct further testing and analysis to investigate conservatism in the stress rupture model and evaluate material age degradation.

Additional analysis of stress rupture life requires understanding the fiber stresses including stress that occurs due to thru-wall composite compression in COPV

components. Data must be obtained at both zero gauge pressure (pre-stress) and at the component operating pressure so that this phenomenon can be properly evaluated. The zero gauge pressure stresses are predominantly a result of the autofrettage process used during vessel manufacture. Determining these pre-stresses and the constitutive behavior of the overwrap at pressure will provide necessary information to better predict the remaining life of the STS COPVs.

The primary test objective is obtaining data to verify the hypothesis of a radially oriented thru-thickness stress-riser in the COPV composite whose magnitude is a function of the applied pressure and the load history. The anticipated load dependent response follows from the constitutive behavior of the composite overwrap so data to quantify its non-linear and time dependent response will be sought.

The objective of the Fiber Braggs Gratings (FBGs) were to advance the state-of-the-art by developing techniques using FBG sensors that are capable of assessing stress-rupture degradation in Kevlar COPVs in a health monitoring mode (1). Moreover, they sought to answer questions of how embedded sensors affect overall integrity of the structure. And lastly, they sought to provide an important link in the overall stress rupture study that will help close the loop on the COPV fabrication process. NDE inspection methods will be used from start to finish and FBG will be an integral link within the overall chain.

Theory of Operation

FBGs work as filters by selecting a certain portion of the input spectrum of light and reflecting it back as shown in figure 1.

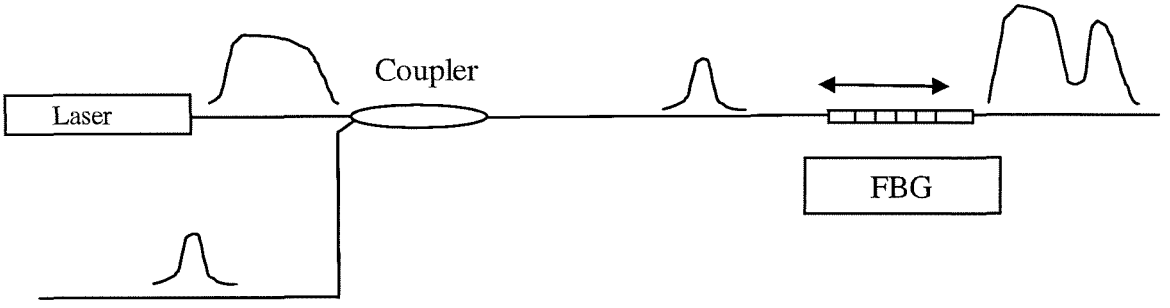

Figure 1. Fiber Braggs Grating Filter

The equation governing the principal of operation is given in equation 1 (2).

$\lambda_G = 2n\Lambda_G$ 1

Here, Λ_G is the grating spacing; n is the refractive index of the material; and λ_G is the Braggs wavelength.

Minimum Bend Radius

Critical radius for single mode fiber: there is a critical radius R_c such that there is significant radial loss for bend radius < R_c,

$$R_c = \frac{3n_1^2}{4\pi\left(n_1^2 - n_2^2\right)^{3/2}}\ \lambda$$

Where n_1 is the refractive index of the core of the fiber, and n_2 is the cladding.

Braggs Maximum Reflectivity

The Maximum reflectivity of a BG at the center of the reflection band-width is given by

$$R_{Max} = \tanh^2 \{(\pi/\lambda_G) \cdot (\delta n) \cdot L\} \quad \ldots\ldots 2$$

λ_G is the Bragg wavelength; δn is the average increase of refractive index by UV light; and L is the length of grating. If we select λ_G = 1300 nm, δn to be 3 x10^{-3}, we can plot R_{Max} as a function of the grating length as seen in the graph below. Graph 1 shows that if L is greater than 270 microns, the reflectivity is100%. It must be pointed out that if L is longer (3-7 mm), the reflected peak gives a better resolution (long grating). If L is close to its theoretical maximum the resolution is less (short grating). However, if the longer gratings are placed on or into a curved surface peak splitting may occur.

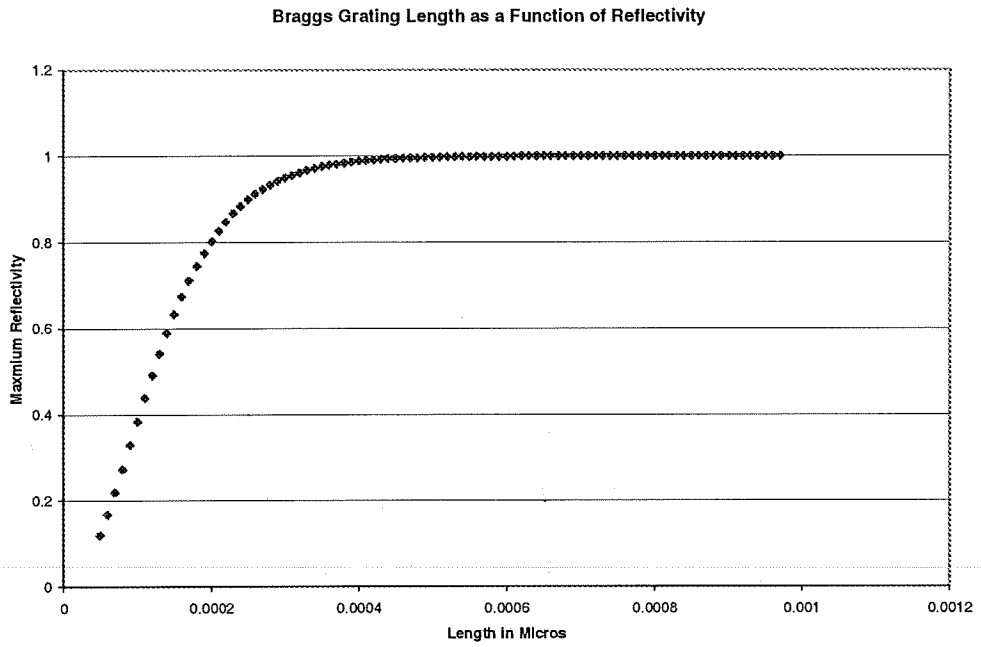

Figure 2, Braggs planes placed inside of fiber optics cable.

Temperature sensor

If we desire to make a temperature sensor, then we can write the change in λ_G as (3),

$$\Delta\lambda_G = \lambda_G \times (\alpha+\xi) \times \Delta T \quad \ldots\ldots 3$$

Here, α is the expansion coefficient of the material. For silica, this value is .55 x 10^{-6}/°C. For GeO_2 dopant, the thermo-optic coefficient, $\xi = 8.3\text{x}10^{-6}$/°C. Therefore, $\Delta\lambda_G/\lambda_G$= (8.85 x$10^{-6}$/°C) x ΔT.

Strain Sensor

If we desire to make a strain sensor (3),

$$\Delta\lambda_G = \lambda_G \times (1-p_e)\varepsilon \quad \ldots\ldots 4$$

Here, p_e is the photo-elastic constant which is related to the Pockel's and Poisson ratio. For silica this value is .22, therefore $\Delta\lambda_G = \lambda_G \times 0.78\varepsilon$.

Both strain and temperature can be separated in a polarization preserving fiber.

Grating Writing

FBGs are manufactured by introducing periodic variations in the refractive index in the longitudinal direction of optical fibers. In order to construct FBGs, optical fibers are doped with photosensitive materials called dopants and exposed to ultraviolet (UV) light with a periodic intensity (1). The photosensitive dopants change their properties

according to the intensity of UV light. This phenomenon is called photorefraction. The reflected portion of the spectrum depends on the geometry and chemistry of the periodic structure of the grating. Thus, if the geometry or chemistry of the FBG changes due to either environmental changes or induced perturbations the wavelength of the reflected light would change accordingly.

Experiment Setup

Fiber Installation

The OMS vessel was instrumented with 36 FBG sensors (figures 3 and 4). Three sensors were placed transverse on the zero axes and three in transverse on the 180 axis. The remainder of the thirty was installed in the longitudinal direction (20 on top and 10 on bottom). Keeping with the last centaur test, FBGs sensors were taped down with several layers of kapton tape for each sensor to reduce peak splitting. Then they were attached to the surface of the vessel using M- Bond GA-2. The surface of the vessel was sanded using a 600 grit sand paper and cleaned with isopropyl alcohol. This was done to insure good adhesion of the optical fiber to the vessel surface. Once all of the sensors were bonded, they were tapped down to prevent any loose fiber from entanglement with other wires on the vessel that might cause the FBG to break. We mounted **L-** shaped connector holders to the vessel surface using double sided tape. This made it easier to connect two 10ft patch cables from the vessel to the FBG interrogation system. The order of each labeled sensor line is noted it the Table 1. The table starts with the sensor number followed by the sensor string. The location, orientation and wrap are listed for each sensor. Lastly, the location for each sensor string as it is connected to the vessel is listed in the columns showing top or bottom for the connections.

BRR FBG Data Acquisition System

The FBG data acquisition system was from Blue Road Research (BRR). The stand along system incorporated a communication laser with a central wavelength around 1500 nm which could scan over a 40 nm bandwidth. The unique design was connected to a multiplexer that accommodated 10 channels for each optical fiber. All connected to a SN9565 XXpc microcomputer with a National Instrument interface card. An associated LabView software program allowed each channel with as many as four sensors to be observed at a time. The

collected data was stored by the computer for further analysis.

The optical fibers sensors were purchase from Micron Optic. Each fiber was design with for three to four sensors. The sensors were separated by five to ten nanometers.

During the burst test, the FBG interrogator was set to scan at 4 Hz. The strain generated in the fiber optic sensors was recorded as wavelength data that was converted to micro-strain and plotted using MS Excel.

Results

The FBG is more of a point sensor; hence it measured localized strain as opposed to a foil strain gauge that covers an area. The area of a foil gauge can be .25 inch square or more which measures the average strain (4). The sensing element in the FBG is on the order of 3 to 7 millimeter. Ideally, the sensing element is on the order of 1 to 1.5 millimeter longer. The sensing is along the direction of light propagation for the FBG.

Therefore, strain tends to be more localized and differ from point to point on a large surface, particular in the case of the surfaces of a composite structure under dynamic loading as in the case of the COPV. Adjacent strains of the material can see different loading.

In Figure 5 we see as example of three different loading levels along the 120 degree line of the top hemisphere, (sensors 3, 4 and 5). The direction of the gauges is along the COPV wrap. The loading is linear with pressure. However, the maximum strain experienced by the sensors are, 13025.5, 8985.0, and 3536.7 (micro strain) while the pressure per square inch experienced was 7586, 76725, and 6613, respectfully. These values are at or near the point where the COPV ruptured, 7667 psi.

One may also note that a brakeage in the plots can be seen. These brakeage can be attributed to several effects; one, it maybe from the onset of the liner beginning to yield to the stress, becoming plastic. Second, underline cracks may have reached some critical load level. Or, underline Kevlar strain(s) giving way and the loading is being transferred to adjacent strains as pressure inside the vessel continued to increase until failure.

The breakage in the data seems to be an onset of a plateau region. The plateau may indicate that the Kevlar has reached its yielding level or the fiber optic cable may have reached its yielding limit.

Similar results can be seen in Figure 6 (sensors 6, 7, and 8). The strain is measured along the 180 degree line on the bottom hemisphere. The maximum strain is compatible to the level measured by sensors 3, 4, and 5. However, sensor 8 failed as the pressure levels read 5300 psi. Here the adhesive may have given way. The COPV was coated with a layer of polyurethane that had been exposed to ultra violet rays for several years. Moreover, flaking of the Polyurethane was noted while applying the FBGs to the COPV. If the epoxy adhesive gave way under stress this would account for the zero loading at this pressure.

Figure 7 represents sensors 16, 17 and 18. These sensors were mounted transverse to the direction of the wrap along the 0 degree line and located on the top hemisphere. The sensors are on wraps 5T, 3T, and 1T. The strain levels in these sensors are generally lower because the loading along the direction of wrap were more than the loading transverse to the wrap.

In Figure 8 we illustrate peek splitting using a long FBG (sensor 19). It is located along the 0 degree line A FBG sensor is prone to splitting if it is placed on a curved surface (4). The BRR FBG interrogator cannot properly track the major peak shift when it is under stress. It sees two peaks from the one sensor. The major peek is at 1530 nm and the minor peek is located 1533 nm. Quantitatively, each sensor follows the increase strain with increase pressure. Hence, it is important to properly balance sensitivity (long Braggs Grating) with peak design requirements.

Finally, Figure 9 shows sensors 29, 30, and 31. Sensors 30 and 31 are located on the 300 degree line in the bottom hemisphere and wraps 15L and 2L, respectfully. Each sensor is well behaved and is linear with increased pressure. The maximum strain experience by sensors 31 is greater than that of sensor 30.

Sensor 29 on the contrary, is located along the 180 degree line in the bottom hemisphere on wrap 4L. It is also well behaved and linear with applied pressure.

The liner yield seems to be absent from these sensors. This may suggest that the yield maybe location sensitive.

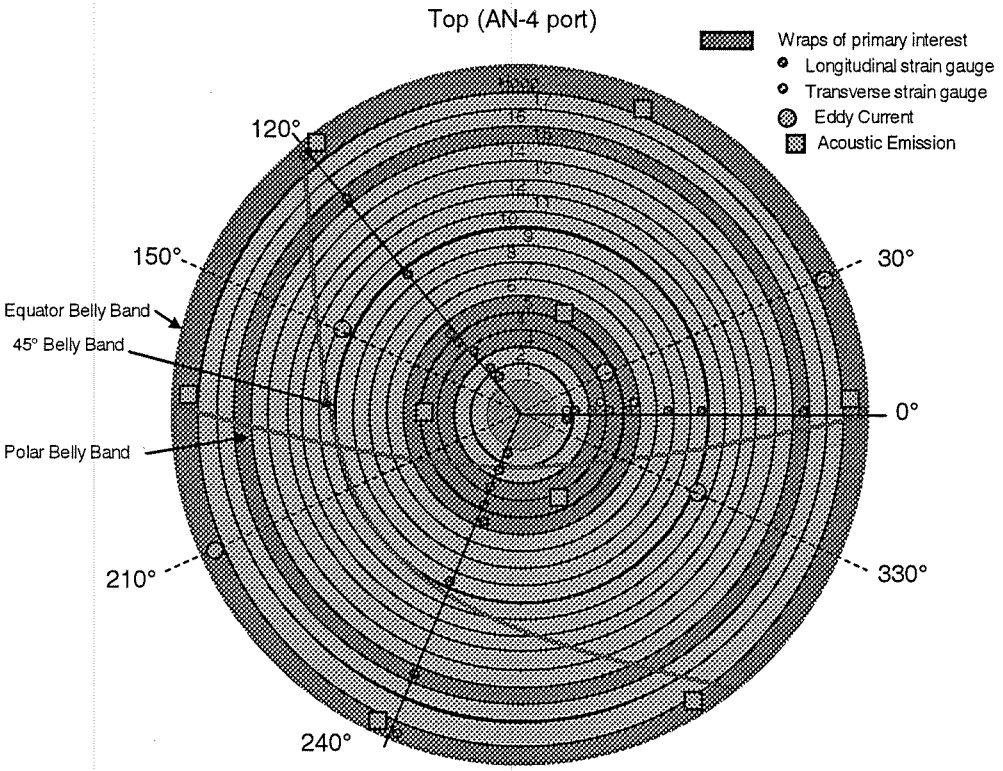

Figure 3. Top view of AN—4 Port

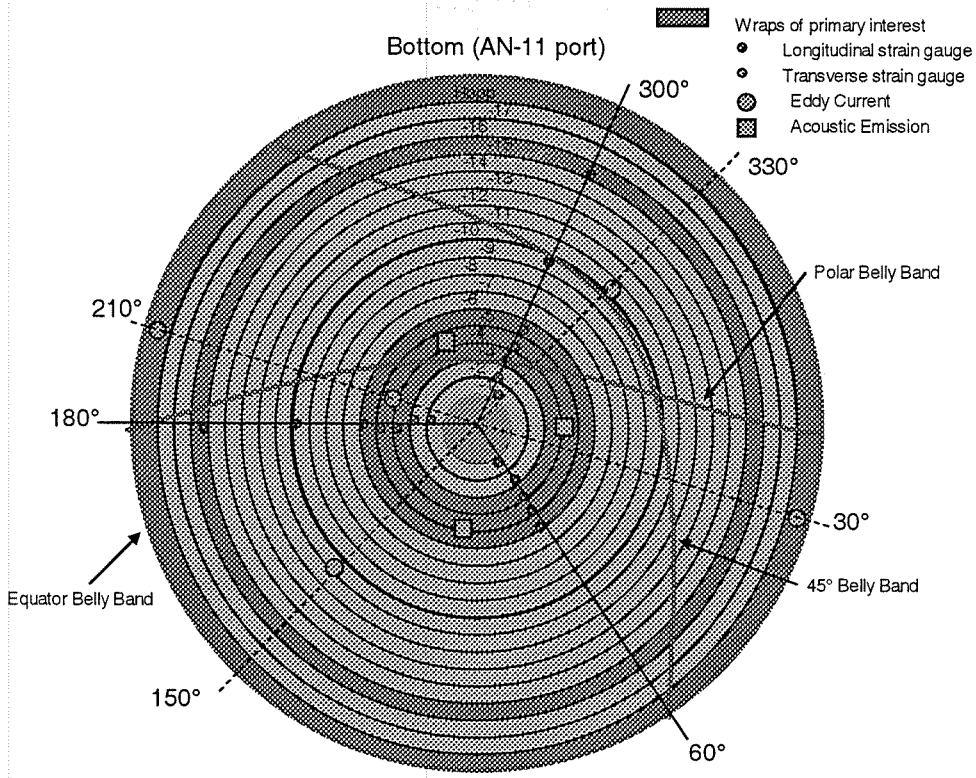

Figure 4. Bottom view of AN—11 Port

Fiber Bragg ID	Switch #, Switch Position**	wavelength (nm)	String #, Line #	Clock Orientation	Arclength to Instrument	Wrap Location	Vessel Hemisphere	Maximum PSI	Passed	Failed	Maximum Micro Strain	Normalized	Channel Normalized
FBG 1	4,2	1544	1a,2 gry	60°	5.63	4 L	B			X			
FBG 2	4,2	1552.5	1a,2 gry	60°	2.75	2 L	B			X			
FBG 3	2,1	1535	2a,1 grn	120°	6.00	4 L	T	7287.3	X		13025.0	100.00	1.000
FBG 4	2,1	1545	2a,1 grn	120°	29.50	HOOP, L	T	7235.0	X		8985.0	68.98	1.450
FBG 5	2,1	1556	2a,1 grn	120°	24.63	15 L	T	6613.0	X		3536.0	27.15	3.684
FBG 6	3,2	1529	3,2 wht	180°	7.50	5 T	B	6248.0	X		10367.0	79.59	1.256
FBG 7	3,2	1540	3,2 wht	180°	4.00	3 T	B	5643.0	X		7131.0	54.75	0.564
FBG 8	3,2	1550	3,2 wht	180°	1.00	1 T	B	5296.0	X		4024.0	30.89	1.000
FBG 9	2,2	1543	4,2 omg	180°	24.25	15 L	B	5685.0	X		1459.0	11.20	2.758
FBG 10	5,2	1548	5,2 blk	60°	23.50	15 L	B	0.0				0.00	
FBG 11	7,1	1530	6,1 gry	240°	7.75	5 L	T	5659.0	X		4246.0	32.60	1.000
FBG 12	7,1	1535	6,1 gry	240°	4.25	3 L	T	5659.0	X		3446.0	26.46	1.232
FBG 13	7,1	1540	6,1 gry	240°	0.50	1 L	T	3395.0	X		2966.0	22.77	1.432
FBG 14	7,1	1545	6,1 gry	240°	2.75	2 L	T	3395.0		?	2147.0	16.48	1.978
FBG 15	7,1	1551	6,1 gry	240°	6	4 L	T	3395.0		?	2281.0	17.51	1.861
FBG 16	1,1	1530	7,1 blu	0°	8.00	5 T	T	7638.0	X		10953.0	84.09	1.000
FBG 17	1,1	1540	7,1 blu	0°	3.88	3 T	T	7079.0	X		7958.0	61.10	1.376
FBG 18	1,1	1550	7,1 blu	0°	1.00	1 T	T	6167.0	X		3395.0	26.07	3.226
FBG 19	1,2	1530	8,1 red	0°	7.50	5 L	T	7587.3		?	12855.0	98.69	
FBG 20	1,2	1535	8,1 red	0°	3.88	3 L	T	7587.0		?	11842.0	90.92	
FBG 21	1,2	1540	8,1 red	0°	1.00	1 L	T	7587.0		?	7911.8	60.74	
FBG 22	1,2	1545	8,1 red	0°	2.50	2 L	T	7587.0		?	3948.6	30.32	
FBG 23	1,2	1551	8,1 red	0°	6.00	4 L	T	3058.0		X		0.00	
FBG 24	4,1	1530	9,1 blk	0°	30.25	HOOP, L	T			X		0.00	
FBG 25	4,1	1535	9,1 blk	0°	21.88	13 L	T			X		0.00	
FBG 26	4,1	1540	9,1 blk	0°	11.50	7 L	T			X		0.00	
FBG 27	4,1	1545	9,1 blk	0°	14.75	9 L	T			X		0.00	
FBG 28	4,1	1550	9,1 blk	0°	25.50	15 T	T		X			0.00	
FBG 29	3,1	1530	10, 1 wht	180°	5.50	4 L	B	7492.0	X		4489.0	34.46	1.998
FBG 30	3,1	1535	10, 1 wht	300°	25.00	15 L	B	7638.0	X		5349.0	41.07	1.677
FBG 31	3,1	1540	10, 1 wht	300°	2.75	2 L	B	7638.0	X		7577.0	58.17	1.184
FBG 32	3,1	1545	10, 1 wht	300°	8.00	5 L	B	7260.0	X		8969.0	68.86	1.000
FBG 33	3,1	1550	10, 1 wht	180°	2.50	2 L	B	7638.0		?	6531.0	50.14	1.373
FBG 34	6,1	1533	11,1 gry	270°	23.50	15 L	T			X		0.00	
FBG 35	6,1	1548	11,1 gry	270°	14.50	9 L	t			X		0.00	
FBG 36	6,1	1553	11,1 gry	270°	29.50	HOOP, L	t			X		0.00	

Table 1. Maximum strain level experience in each sensor. Some of the sensors fail and others were subject to surface or adhesion issues. The sensors with a '?' beside them represents peak splitting (and/or other issues) that made the data difficult to interpret.

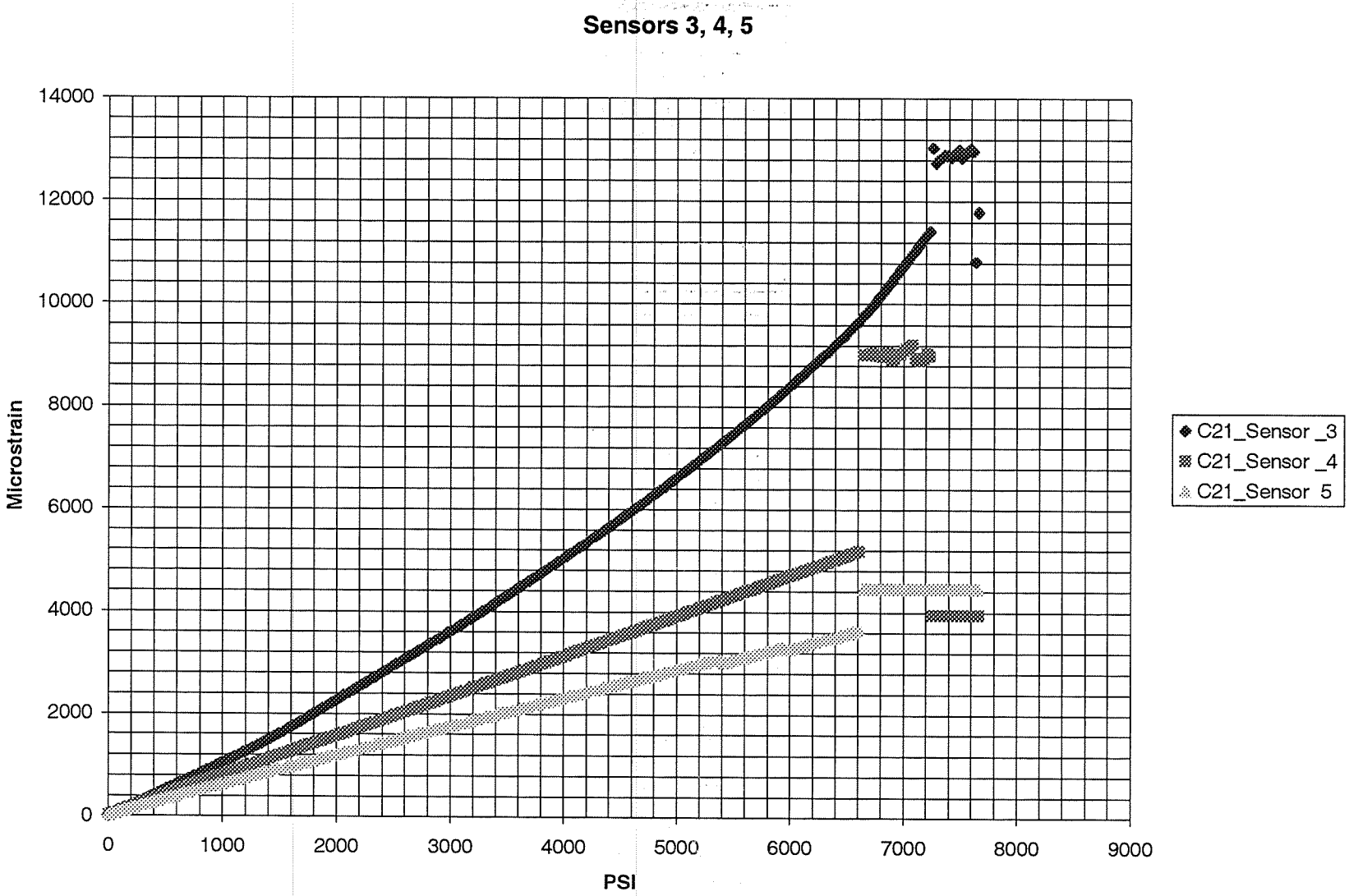

Figure 5. FBG sensors 3, 4 and 5 showing onset of liner yield. Sensors are located in the top hemisphere on wraps 4L, HL, and 15L along the 120 degree line.

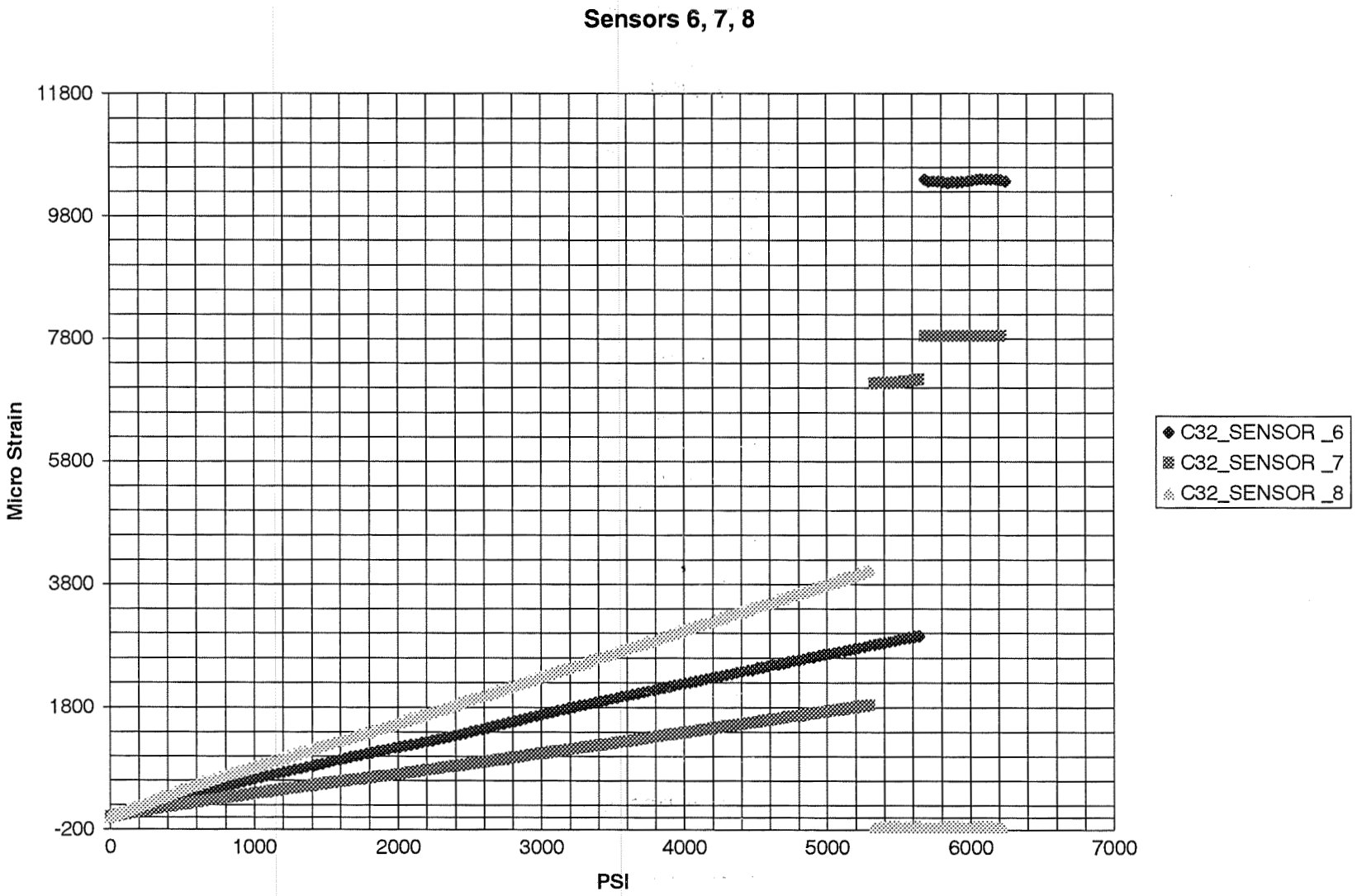

Figure 6. FBG sensors 6, 7 and 8 showing onset of liner yield. Sensor 8 failed above 5250 psi. The failure may be due to adhesive related problems or underline polyurethane. Sensors are located in the bottom hemisphere on wraps 5T, 3T, and 1T along the 180 degree line.

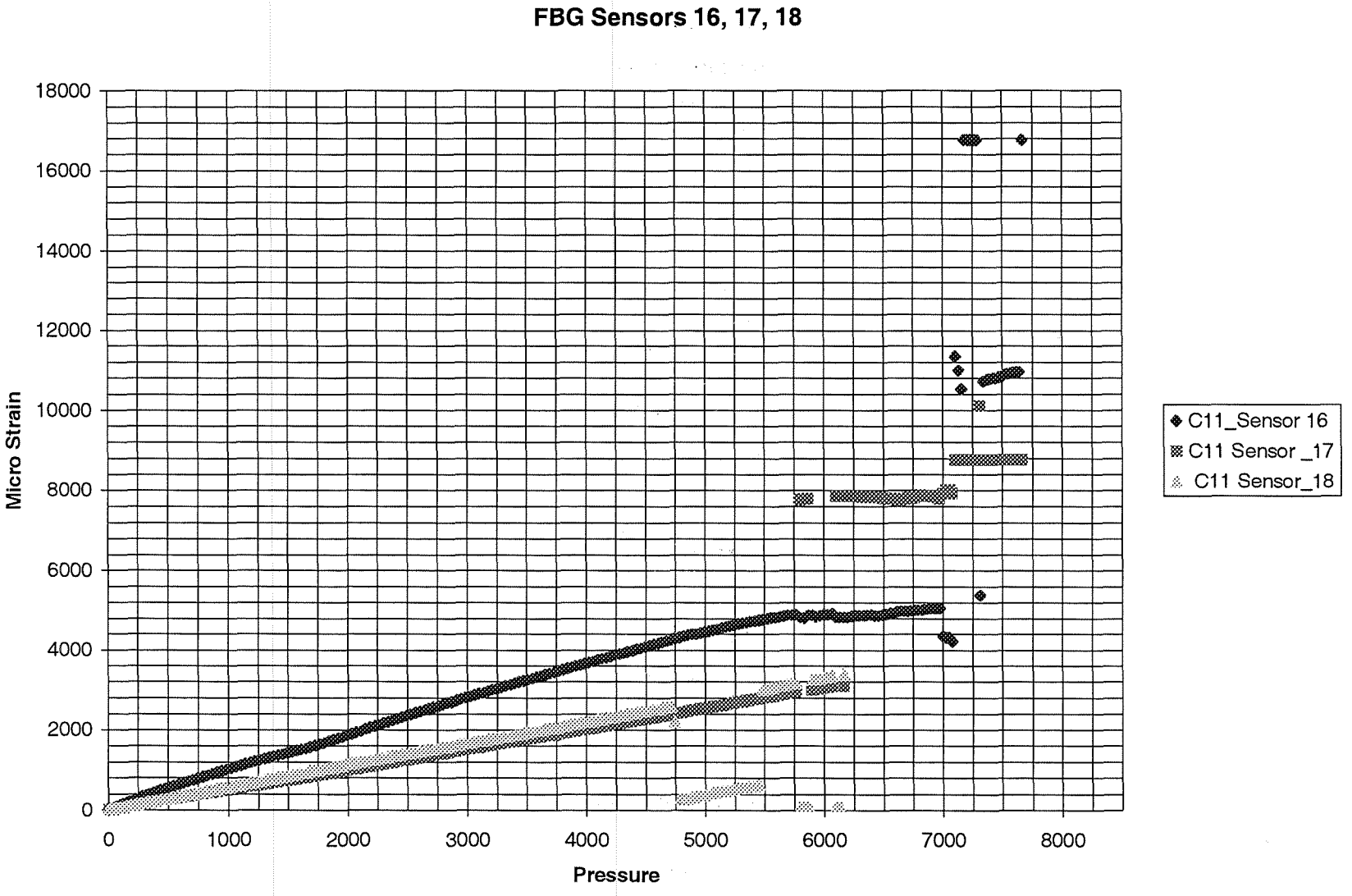

Figure 7. Sensors 16, 17 and 18 were attached transverse to the wrap direction. Ideally, the stress generated in the Kevlar wrap is smaller than along the wrap. Sensors are located in the top hemisphere on wraps 5T, 3T, and 1T along the 0 degree line.

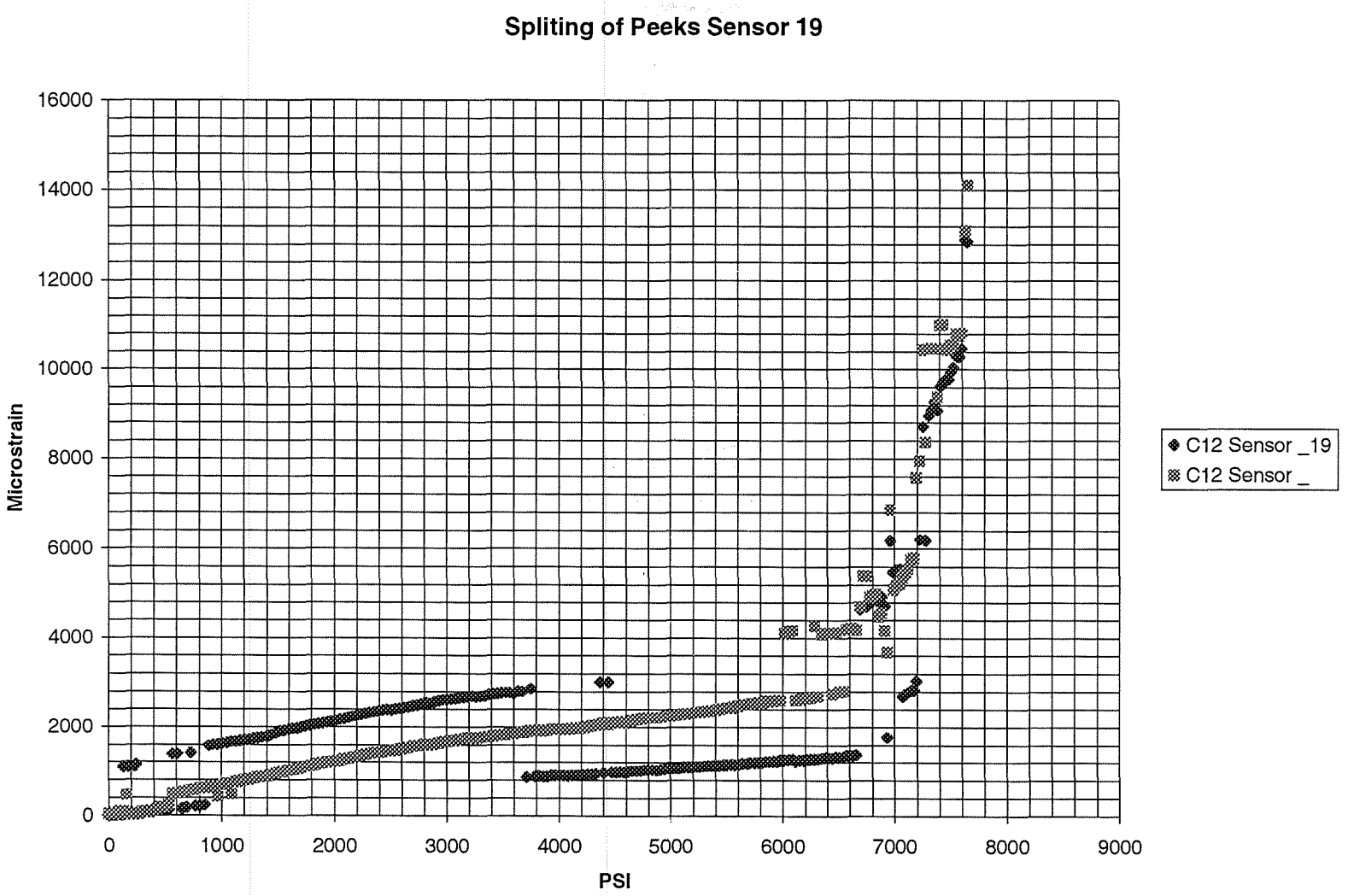

Figure 8. Sensor 19 shows that splitting can occur if the FBG if the sensor is placed on curved surfaces. The splitting makes difficult to interpret the underlying strain. Sensor is located in the top hemisphere on wraps 5L alone the 0 degree line.

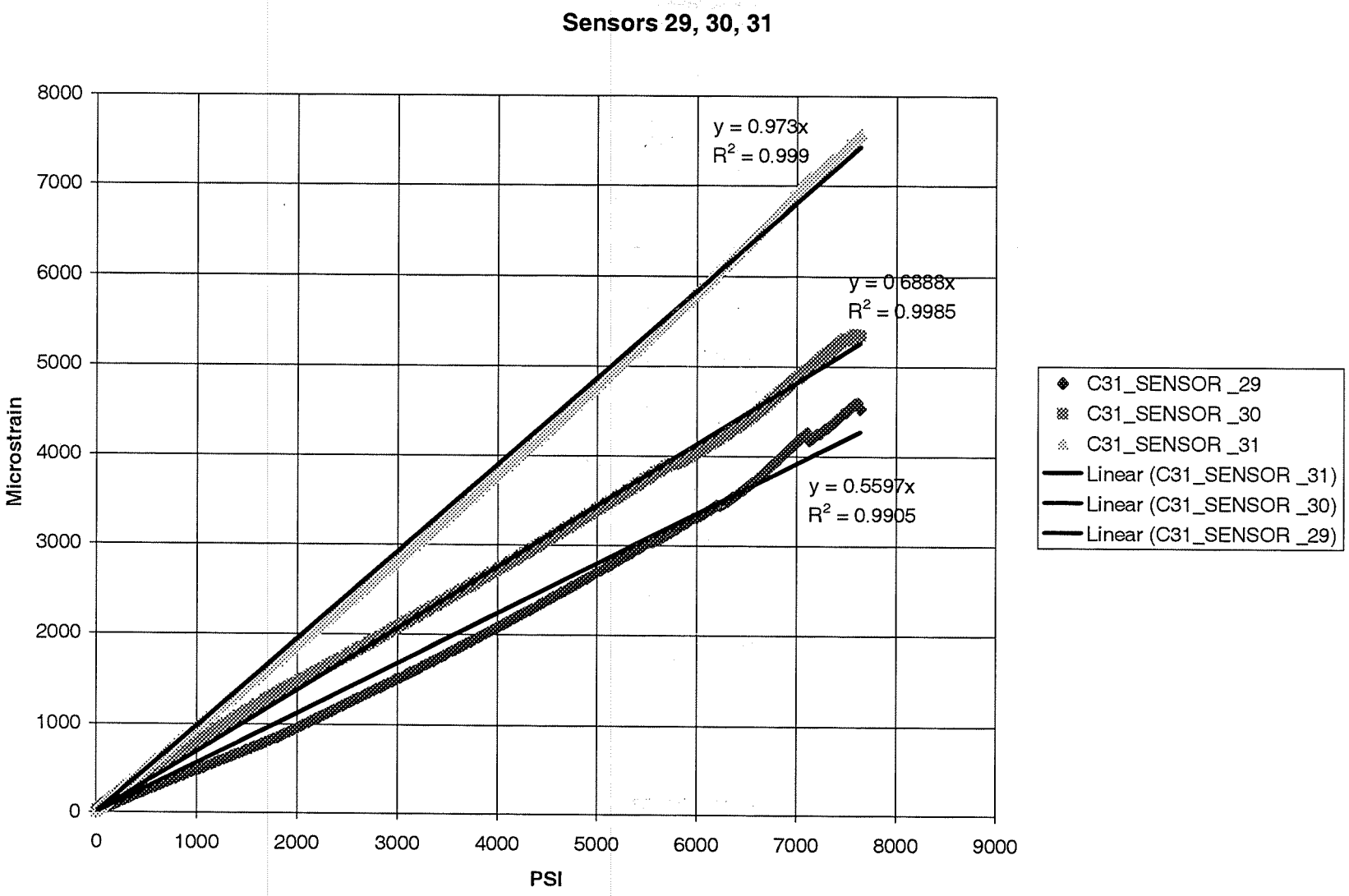

Figure 9. Sensors 29, 30 and 31 were behaved. The liner yield seems to be absent from these sensors. Sensors are located in the bottom hemisphere on wraps 4L 180 degree for sensor 29 and wraps 2L and 5L alone the 300 degree line for 30 and 31.

Conclusion

We evaluated the performance of Fiber Braggs Grating (FBG) sensors for NDE application by hydrostatically pressurizing a Space Transportation System (STS) 40-inch Kevlar® Composite Overwrapped Pressure Vessel (COPV).

Generally, the FBG sensors performed as expected. They were able to detect the onset of yield in the titanium liner. The pressure at yielding was different at different locations. However, it appears that the onset was 5500-6500 psi. Once the Kevlar overwrap reached its dynamic limit; it reached a plateau, but gave way to increased pressure build up in the vessel.

Some of the FBG sensor failed for various reasons: splitting because of uneven surfaces, adhesion due to surface preparation or underline cracks in the polyurethane that covered the Kevlar strands or unknown. Generally, they showed a linear relationship with applied pressure.

1. Distributed sensing of carbon-epoxy composites and pressure wound vessels using fiber Bragg gratings, Smart Materials 2003: Smart Sensor Technology and Measurement Systems, J. Grant, R. K. Kaul, S. L. Taylor, G. Myers, C. E. Wilkerson, K. V. Jackson, NASA Marshall Space Flight Ctr.; A. Sharma, Alabama A&M Univ. Proceedings of SPIE Vol. 5050 (2003), 187
2. Bennion, J.A.R. Williams, L. Zhang, K. Sugden, and N.J. Doran, "UV-written in-fiber Bragg gratings", Optical and Quantum Electronics. **28**, 93 (1996)
3. Lo YL. Using in fiber Braggs-grating sensors for measuring axial strain and temperature simultaneously on surfaces of structures. Opt. Engng 1998;37 (8):2272-6
4. Kang, H. Park, J. Kang, D. Kim, C. Hong, C. and Kim, C. " Strain Monitoring of a Filament wound Composite Tank using Fiber Braggs Grating Sensors" Smart Mater. Strut. **11** (2002) 848-853